TM-720
2941.000

fermi national accelerator laboratory

WIDE-BAND SINGLE HORN SYSTEM (II)

S. Mori

February 16, 1977

INTRODUCTION

A simpler wide-band horn system has been proposed in TM-663[1]. In this report, recent studies about the straight-cone, single-neck horn system (see Figure 1 in TM-663) are discussed. The inner radius of a narrow-neck is maintained at 1cm, which is of sufficient width to be protected from the high intensity, high energy beam. Neutrino and anti-neutrino fluxes, and wrong sign backgrounds with and without an anti-neutrino plug, are compared for the present double horn system and various single horn arrangements at the incident proton energy of 400 GeV. In conclusion, a single horn system can be as short as 2m and is enormously advantageous from the standpoints of construction economy and of saving high radiation exposure during maintenance.

FOCUSSING PROPERTIES BY HORNS

For secondary particles of transverse momentum P_T (GeV/c), the optimum point-to-parallel focussing condition between the horn current I (kA) and slope α (mrad) is given by

$$\alpha I = 16.33\ P_T$$

for the straight-slope, single-neck horn system[2] Figures 1 and 2 show computed pion and kaon spectra for 400 GeV incident protons, as functions of momenta and angles. Parameterization by Stefanski and White[3] was used throughout the present analyses[4]. The average P_T for pions is about 0.3 GeV/c, with a wide range of momenta, but the average value for kaons seems to be considerably larger. Therefore, the single-neck horn system cannot be simultaneously optimized for neutrinos from pion decays (low energy neutrinos) and for neutrinos from kaon decays (high energy neutrinos). For example, Figures 3 (a), (b), (c), (d), (e) and (f) show computed neutrino fluxes for a horn of α = 30 mrad as a function of I (kA) at the neutrino energies of 20, 30, 50, 100, 150 and 200 GeV, respectively. Three curves correspond to three target positions, i.e., 2.42, 5.42 and 8.42m from the upstream end of the horn. The length of the horn is 3.68m, the same as the present upstream horn. From these figures, it can easily be seen that neutrino spectra can be adjusted by horn excitation current to some extent.

TARGET POSITIONS AND HORN LENGTHS

As seen in Figure 3, the neutrino flux depends somewhat upon the target position. It is particularly important in order to suppress the wrong sign background without using a plug. Since the secondary particles produced in the forward direction within a solid angle subtended by the horn neck are not focussed nor defocussed by the horn, the wrong sign background is expected to be larger when the target is placed closer to the horn neck of 1cm radius. Figures 4 and 5 show computed neutrino fluxes and wrong sign backgrounds for a horn of α = 30 mrad as a function of the horn length at the neutrino energies of 20, 30, 50, 100, 150 and 200 GeV.[5] The target position is fixed at 5.42m and the horn current is 140 kA. The neutrino fluxes are essentially constant for the horn length longer than 2m, but the wrong sign backgrounds decrease monotomically as the horn lengthens. This is due to the change in the solid angle subtended by the horn neck. Figures 6 and 7 show similar curves for the anti-neutrino. No plug is used.

Figures 8 and 9 show computed neutrino fluxes and wrong sign backgrounds for five horn lengths of 1.68, 1.93, 2.18, 3.68 and 6.18m as a function of the distance between the target and the downstream of the horn where the horn neck is situated. The horn slope is 30 mrad and the horn current is 140 kA. Both the fluxes and backgrounds are essentially identical for the horns longer than 2m. Namely, the horn can be as short as 2m compared to the total horn length of 9.16m for the present double horn system. The wrong sign backgrounds decrease as the target distance increases.

RADIUS OF THE OUTER CONDUCTOR

It seems to be quite safe to assume that very low energy secondary particles, for example, below 20 GeV, can be ignored in the wide band neutrino train at Fermilab. Then, the production angle to be covered is roughly 0.3/20 = 15 mrad. It was shown that neutrino or anti-neutrino fluxes from secondary particles produced with polar angles greater than 16 mrad are essentially zero for all horn systems considered in this analysis, which includes the present horn system. Therefore, the radius of the outer conductor can be 0.015 x 1200 = 18cm. The distance between the target and the downstream of the horn is assumed to be 12m or less.

NEUTRINO BEAM

Figure 10 shows computed neutrino fluxes for the present double horn system and four single horn arrangements at the incident proton energy of 400 GeV. Circle points correspond to the horn of 30 mrad cone slope and 2.18m in length. Other single horns are 3.68m long, the same as the present upstream horn. Two spectra are shown for the horn of a cone slope of 17 mrad, at the horn currents of 75 and 120 kA. Since the maximum current is likely to be limited, it is advantageous to build a small slope horn in order to enhance higher energy neutrinos.

Table I gives relative integrated neutrino event rates. The total cross section for neutrino interactions was assumed to be proportional to the neutrino energy. As discussed in TM-663, neutrino flux differences between any single horn system and the present double horn system become smaller at higher incident proton energies.

Wrong sign backgrounds are also shown in Figure 10. As discussed above, when the plug is not used, the backgrounds are determined by the solid angle subtended by the horn neck.

ANTI-NEUTRINO BEAM

Figure 11 shows computed anti-neutrino fluxes and wrong sign backgrounds for the present double horn system and the single horn systems of a cone slope of 30 mrad at the incident proton energy of 400 GeV. No anti-neutrino plug is used. The single horn system of 30 mrad cone slope and 2.18m length gives very similar neutrino flux and background as the present double horn system.

To reduce the wrong sign background, an anti-neutrino plug can be used. In this case, the computed fluxes and backgrounds are relatively sensitive to the angular step used in the NUADA program and also to the dimension of the plug. In order to reduce computational errors and to make reasonable comparison for various horn systems, anti-neutrino fluxes and wrong sign backgrounds were computed for several plugs of different radii. The results are shown in Figures 12 through 17 for the present double horn system (140 kA); the present upstream horn alone at the target positions of 2.42m (present position) and 5.42m (140 kA); the single horns of 30 mrad cone slope of 3.68m and 2.18m lengths at the target positions of 5.42m and 9.42m, respectively (140 kA); and the single horn of 17 mrad cone slope at the target position of 5.42m (75 kA). Since it is rather difficult to build a reliable plug of a small radius, the practical plug radius should be assumed to be 1.4cm or larger.

Table II summarizes relative integrated anti-neutrino event rates and wrong sign background (neutrino) event rates in the energy range up to 150 GeV, for the present double horn system and three single horn arrangements. The total cross sections for anti-neutrino and neutrino interactions were assumed to be proportional to their energies and, furthermore, to be equal. Since the neutrino cross section is larger by a factor of about three at lower energies than the anti-neutrino cross section, the wrong sign background rates should be worsened by the same factor. In general, straight-cone, single horn systems yield substantially larger anti-neutrino fluxes, but wrong sign backgrounds are also larger. Although any detailed comparison should not be made because of computational uncertainty, the upstream horn alone at the target position of 5.42m (140 kA) seems to provide nearly as good background rejection as the present double horn system and, furthermore, it seems to give much better flux.

CONCLUSIONS

The simpler single horn system can provide adequate neutrino and anti-neutrino fluxes. The horn can be as short as 2m. It will be enormously advantageous from the standpoints of construction economy and maintenance. Since the neck radius must be kept large enough for beam protection, the anti-neutrino wrong sign backgrounds are relatively large when the plug is used.

It must be pointed out that estimates of the neutrino and anti-neutrino fluxes for the single horn system are far more reliable than those for the present horn system. Since the focussing properties for the single horn system are transparent and predictable, neutrino or anti-neutrino beam spectra can be hardened to some extent.

REFERENCES

1. S. Mori, Wide-Band Single Horn System, TM-663, May, 1976

2. R. B. Palmer, CERN 65-32, 141, December, 1965

3. R. J. Stefanski and H. B. White, Jr., FN292, 2060.000, 1976

4. D. C. Cary and V. A. White, Fermilab Internal Report, NUADA, June, 1975

5. Abrupt changes of the neutrino fluxes seem to be due to computational uncertainties from the finite angle step.

TABLE I

RELATIVE NEUTRINO EVENT RATES (%)

HORN ARRANGEMENTS	0 TO 250	0 TO 50	50 TO 100	100 TO 150	150 TO 250
Present Double Horns 140 kA	100.0	57.8	23.1	10.6	8.5
Present Upstream Horn T = 5.42m 140 kA	69.1	33.5	18.8	8.3	8.5
30 mrad 3.68m long 140 kA T = 5.42m	86.0	46.7	21.8	9.7	7.8
30 mrad 2.18m long 140 kA T = 9.42	82.2	43.6	21.4	9.5	7.7
17 mrad 3.68m long 75 kA T = 5.42m	78.0	41.5	20.0	8.8	7.3

NOTE: T = Distance between the target and the upstream of the horn.

TABLE II

RELATIVE ANTI-NEUTRINO EVENT RATES (%) AND WRONG SIGN BACKGROUND RATES WITH A PLUG

	ENERGY RANGE (GeV)			
HORN ARRANGEMENT	0 TO 150	0 TO 50	50 TO 100	100 TO 150
Present Double Horns 140 kA	100.0 (3.0)	82.1 (2.0)	14.5 (6.5)	3.5 (13.2)
Present Upstream Horn 140 kA T = 5.42m	114.9 (3.9)	89.5 (2.9)	20.3 (6.7)	5.1 (11.0)
30 mrad 3.68m long 140 kA T = 5.42m	140.3 (5.7)	112.0 (3.3)	22.6 (14.3)	5.7 (17.9)
30 mrad 2.18m long 140 kA T = 9.42m	156.6 (6.8)	120.4 (4.5)	29.4 (13.9)	6.8 (17.3)

NOTES:

1. The radius of the plug is 1.4cm.
2. T is the distance between the target and the upstream of the horn.
3. Values in parentheses are the ratios of the anti-neutrino events to background events.

FIGURE CAPTIONS

Figure 1: Computed pion spectra for 400 GeV protons on a one interaction length target. Parameterization by Stefanski and White was used.

Figure 2: Computed kaon spectra for 400 GeV protons on a one interaction length target. Parameterization by Stefanski and White was used.

Figure 3: Neutrino fluxes for 400 GeV protons as a function of the horn excitation current in the single horn system of the 30mrad cone slope.

Figure 4: Neutrino fluxes for 400 GeV protons as a function of the horn length in the single horn system of the 30mrad cone slope.

Figure 5: Wrong sign backgrounds for neutrinos for 400 GeV protons as a function of the Horn length in the single horn system of the 30mrad cone slope. No plug is used.

Figure 6: Anti-neutrino fluxes for 400 GeV protons as a function of the Horn length in the single horn system of the 30mrad cone slope.

Figure 7: Wrong sign backgrounds for anti-neutrinos for 400 protons as a function of the horn length in the single horn system of the 30mrad cone slope. No plug is used.

Figure 8: Neutrino fluxes for 400 GeV protons as a function of the target position in the single horn system of the 30mrad cone slope.

Figure 9: Wrong sign backgrounds for neutrinos for 400 GeV protons as a function of the target position in the single horn system of the 30mrad cone slope.

FIGURE CAPTIONS

Figure 10: Neutrino fluxes and wrong sign backgrounds for 400 GeV protons. No plug is used.

Figure 11: Anti-neutrino fluxes and wrong sign backgrounds for 400 GeV protons. No plug is used.

Figure 12: Anti-neutrino fluxes and wrong sign backgrounds for 400 GeV protons as a function of the plug radius in the present double horn system.

Figure 13: Anti-neutrino fluxes and wrong sign backgrounds for 400 GeV protons as a function of the plug radius in the upstream horn (single) system. The target position is 2.42m, the same as the present position.

Figure 14: Anti-neutrino fluxes and wrong sign backgrounds for 400 GeV protons as a function of the plug radius. The target position is 5.42m.

Figure 15: Anti-neutrino fluxes and wrong sign backgrounds for 400 GeV protons as a function of the plug radius in the single horn system of the 30mrad cone slope, and 3.68m in length. The target position is 5.42m.

Figure 16: Anti-neutrino fluxes and wrong sign backgrounds for 400 GeV protons as a function of the plug radius in the single horn system of the 30mrad cone slope and 2.18m in length. The target position is 9.42m.

Figure 17: Anti-neutrino fluxes and wrong sign backgrounds for 400 GeV protons as a function of the plug radius in the single horn system of the 17mrad cone slope and 3.68m in length. The target position is 5.42m.

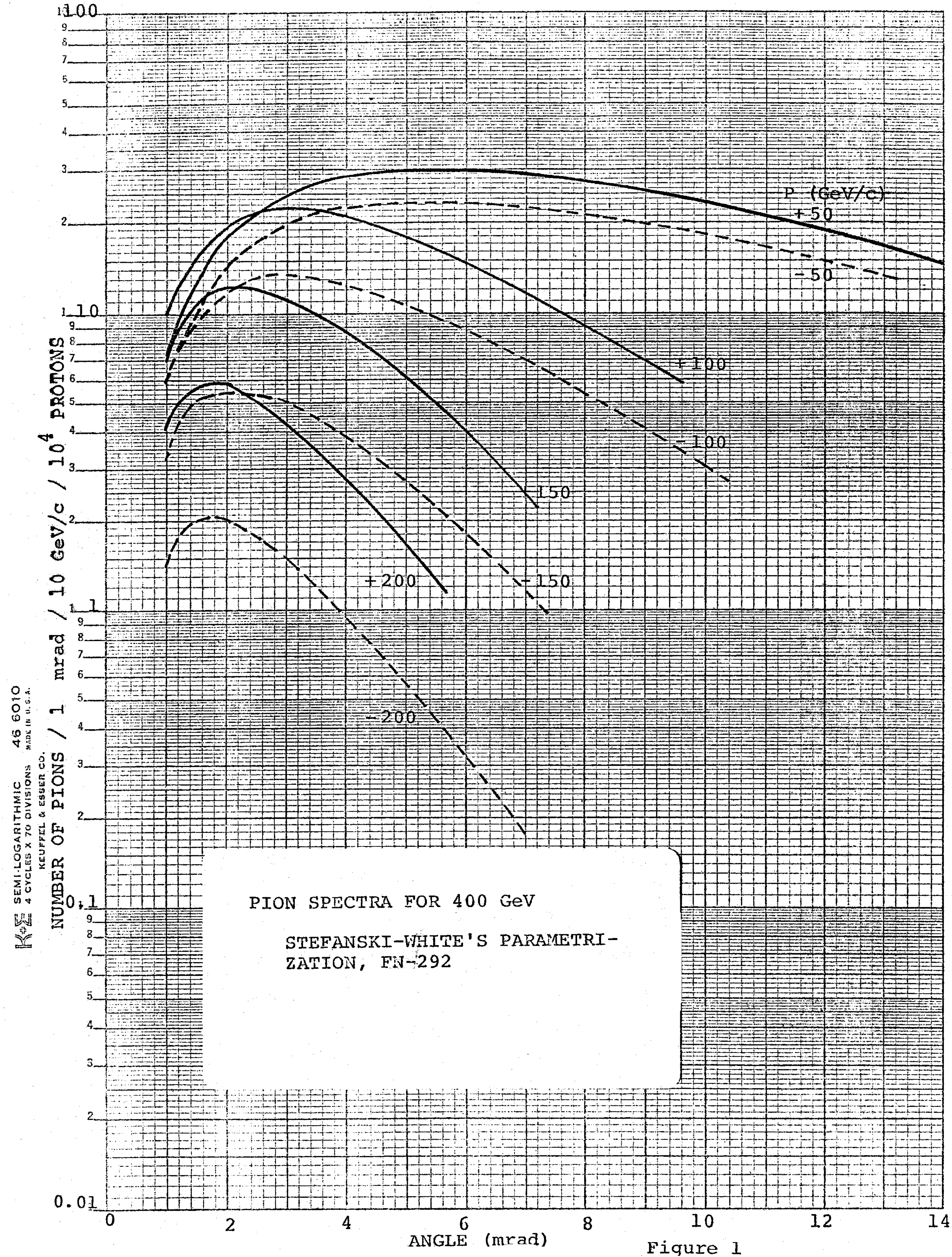
100
10
1
0.1
0.01
0
2
4
6
8
10
12
14
P (GeV/c)
+50
-50
+100
-100
150
-150
+200
-200
NUMBER OF PIONS / 1 mrad / 10 GeV/c / 10^4 PROTONS
ANGLE (mrad)
PION SPECTRA FOR 400 GeV
STEFANSKI-WHITE'S PARAMETRIZATION, FN-292
SEMI-LOGARITHMIC 46 6010
4 CYCLES X 70 DIVISIONS MADE IN U.S.A.
KEUFFEL & ESSER CO.

Figure 1

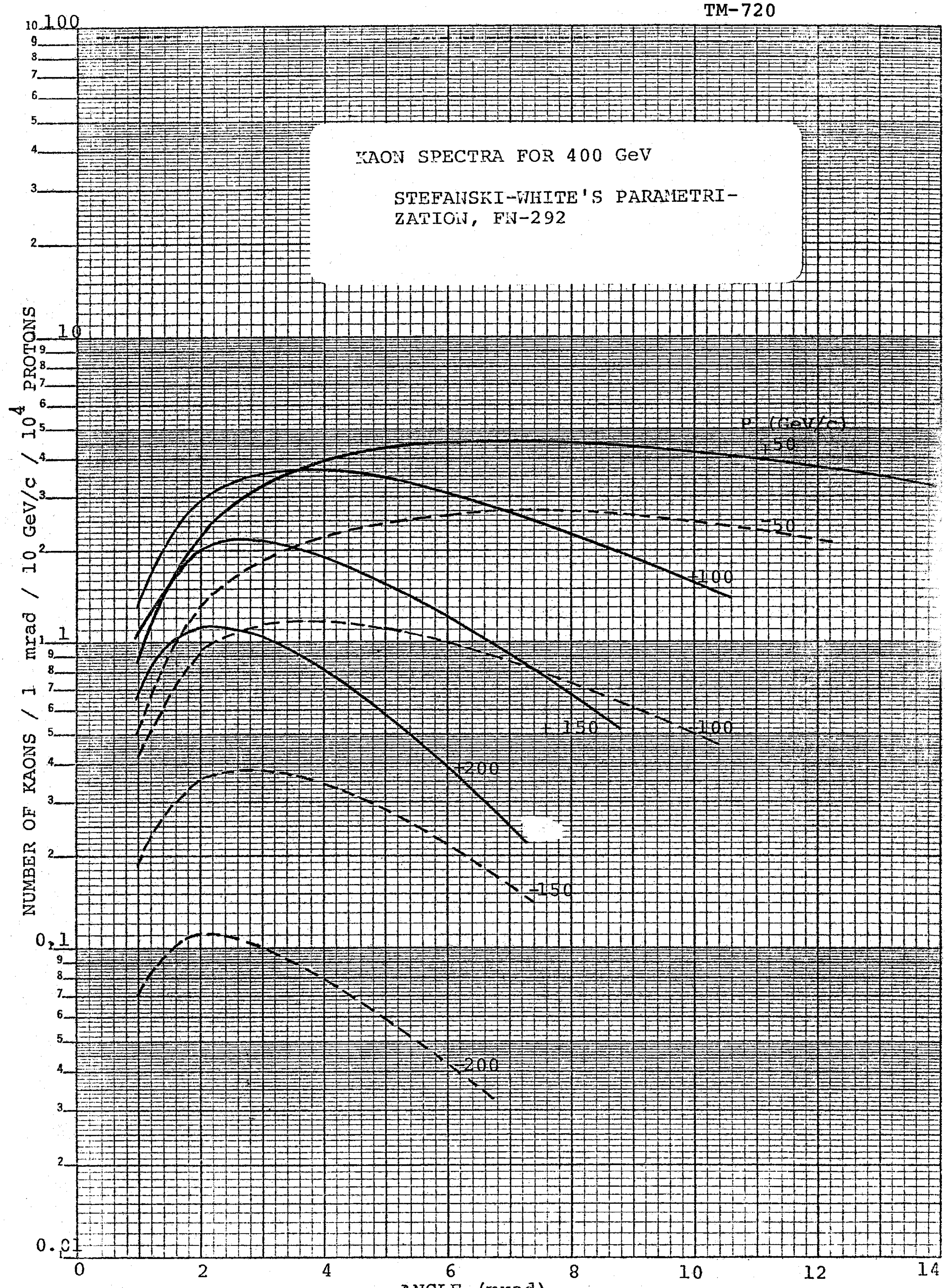
KAON SPECTRA FOR 400 GeV
STEFANSKI-WHITE'S PARAMETRIZATION, FN-292
P (GeV/c)
+50
-50
+100
-100
+150
+200
-150
-200
NUMBER OF KAONS / 1 mrad / 10 GeV/c / 10^4 PROTONS
ANGLE (mrad)
100
10
1
0.1
0.01
0
2
4
6
8
10
12
14

Figure 2

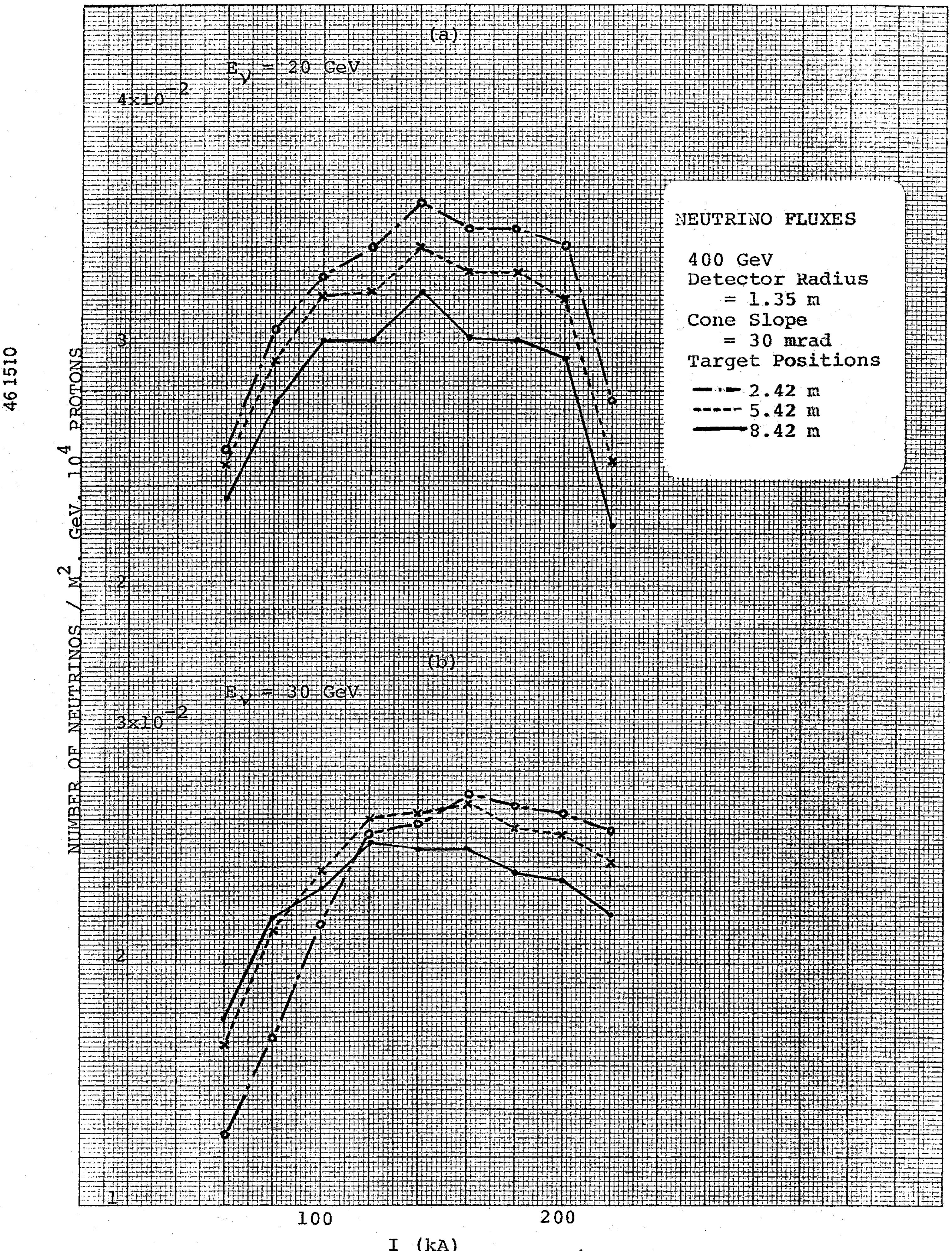
(a)
$E_\nu = 20$ GeV
4×10^{-2}
3
2
NEUTRINO FLUXES
400 GeV
Detector Radius
= 1.35 m
Cone Slope
= 30 mrad
Target Positions
2.42 m
5.42 m
8.42 m
NUMBER OF NEUTRINOS / M^2 · GeV · 10^4 PROTONS
(b)
$E_\nu = 30$ GeV
3×10^{-2}
2
1
100
200
I (kA)
46 1510

Figure 3

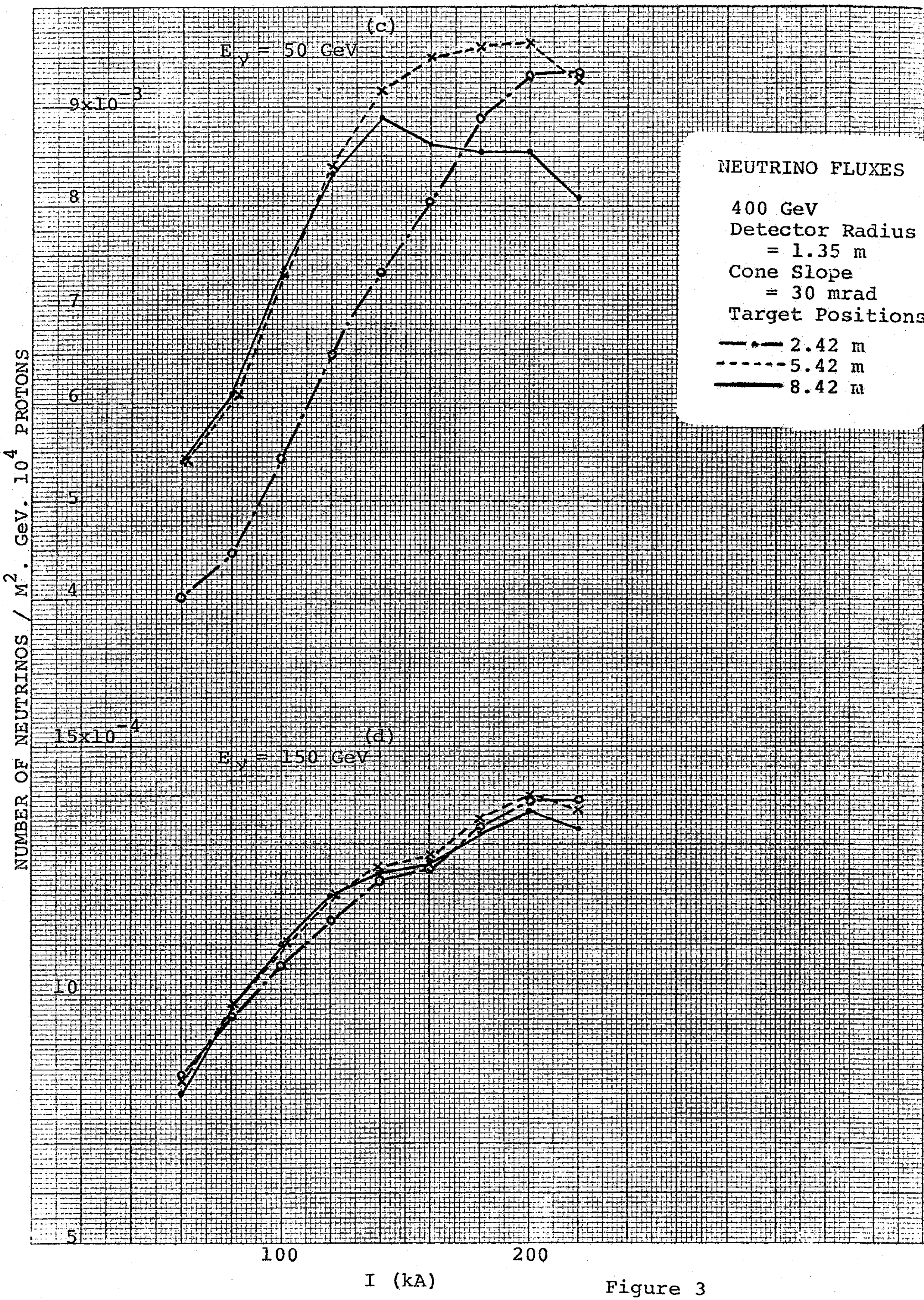
(c)
E_ν = 50 GeV
9x10^{-3}
8
7
6
5
4
NUMBER OF NEUTRINOS / M^2. GeV. 10^4 PROTONS
(d)
E_ν = 150 GeV
15x10^{-4}
10
5
100
200
I (kA)
NEUTRINO FLUXES
400 GeV
Detector Radius
= 1.35 m
Cone Slope
= 30 mrad
Target Positions
2.42 m
5.42 m
8.42 m

Figure 3

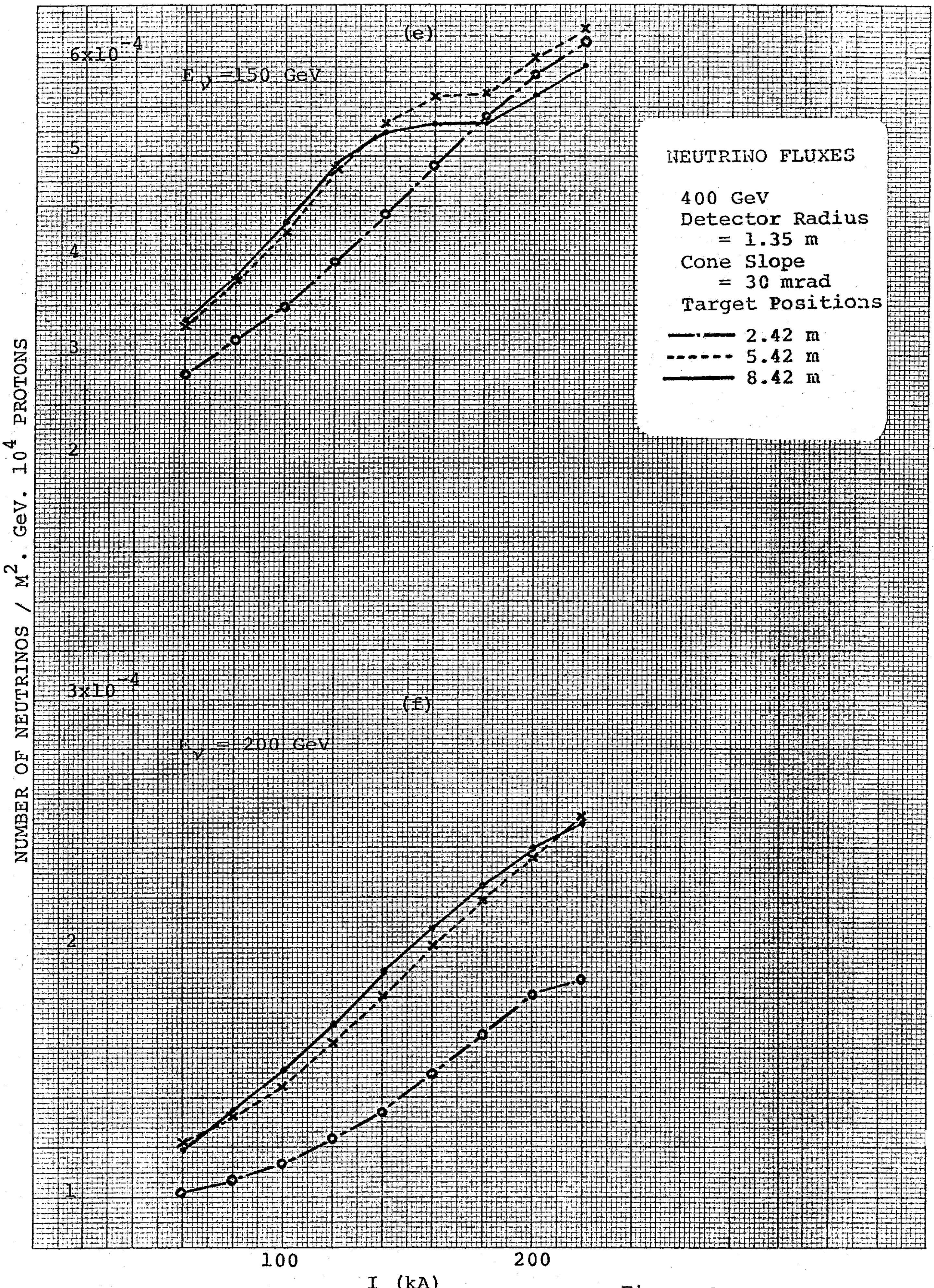

(e)
6×10^{-4}
$E_\nu = 150$ GeV
5
4
3
2
NEUTRINO FLUXES
400 GeV
Detector Radius
= 1.35 m
Cone Slope
= 30 mrad
Target Positions
2.42 m
5.42 m
8.42 m
NUMBER OF NEUTRINOS / M^2. GeV. 10^4 PROTONS
3×10^{-4}
(f)
$E_\nu = 200$ GeV
2
1
100
200
I (kA)

Figure 3

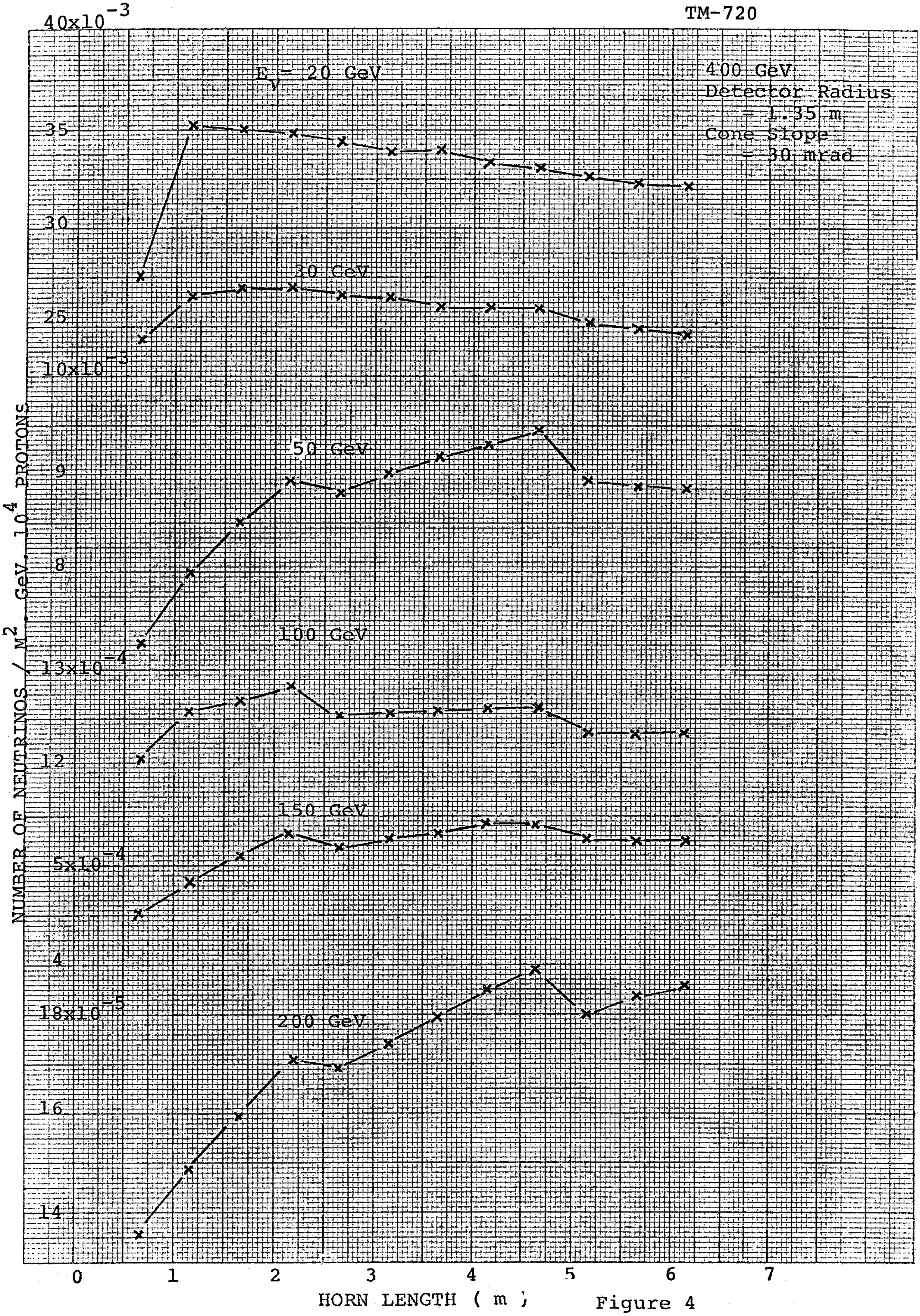

40x10^-3
35
30
25
10x10^-3
9
8
13x10^-4
12
5x10^-4
4
18x10^-5
16
14
E_ν = 20 GeV
30 GeV
50 GeV
100 GeV
150 GeV
200 GeV
400 GeV
Detector Radius
= 1.35 m
Cone Slope
= 30 mrad
NUMBER OF NEUTRINOS / M^2 . GeV. 10^4 PROTONS
0
1
2
3
4
5
6
7
HORN LENGTH (m)

Figure 4

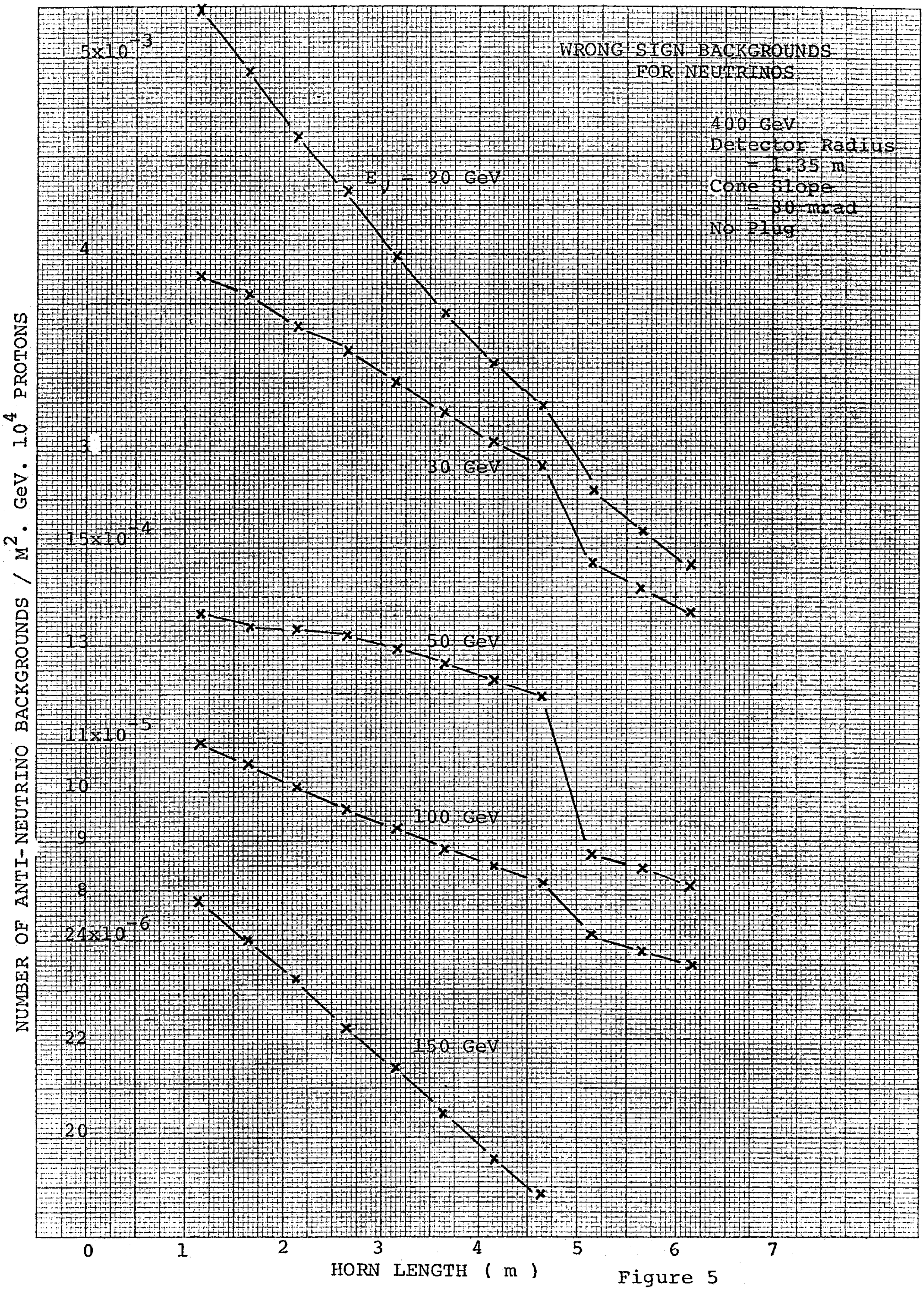
WRONG SIGN BACKGROUNDS
FOR NEUTRINOS
400 GeV
Detector Radius
= 1.35 m
Cone Slope
= 30 mrad
No Plug
E_ν = 20 GeV
30 GeV
50 GeV
100 GeV
150 GeV
5×10^{-3}
4
3
15×10^{-4}
13
11×10^{-5}
10
9
8
24×10^{-6}
22
20
NUMBER OF ANTI-NEUTRINO BACKGROUNDS / M^2. GeV. 10^4 PROTONS
0
1
2
3
4
5
6
7
HORN LENGTH (m)

Figure 5

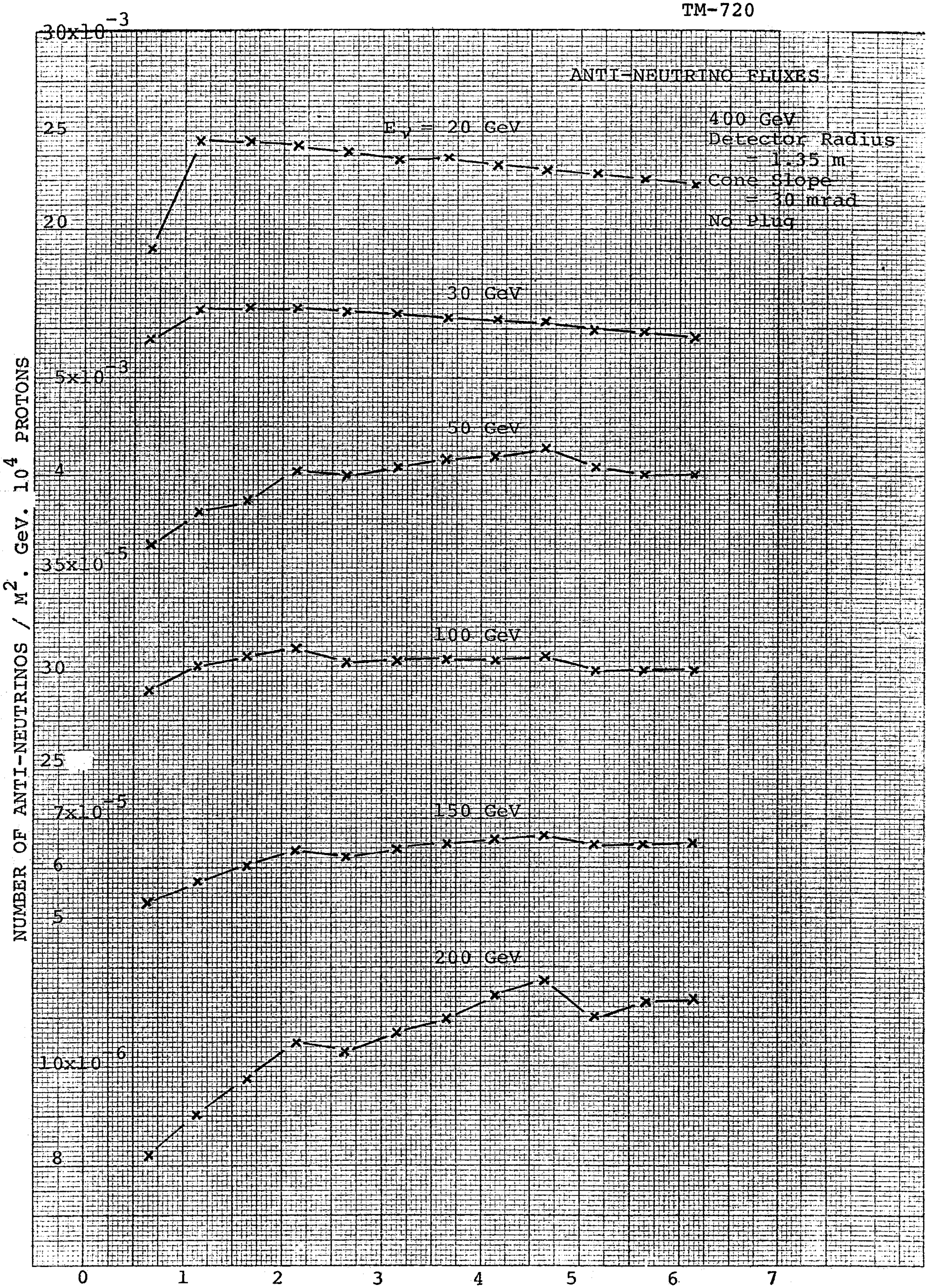
ANTI-NEUTRINO FLUXES
400 GeV
Detector Radius
= 1.35 m
Cone Slope
= 30 mrad
No Plug
$E_{\bar{\nu}}$ = 20 GeV
30 GeV
50 GeV
100 GeV
150 GeV
200 GeV
30x10^{-3}
25
20
5x10^{-3}
4
35x10^{-5}
30
25
7x10^{-5}
6
5
10x10^{-6}
8
0
1
2
3
4
5
6
7
NUMBER OF ANTI-NEUTRINOS / M^2. GeV. 10^4 PROTONS
HORN LENGTH (m)

Figure 6

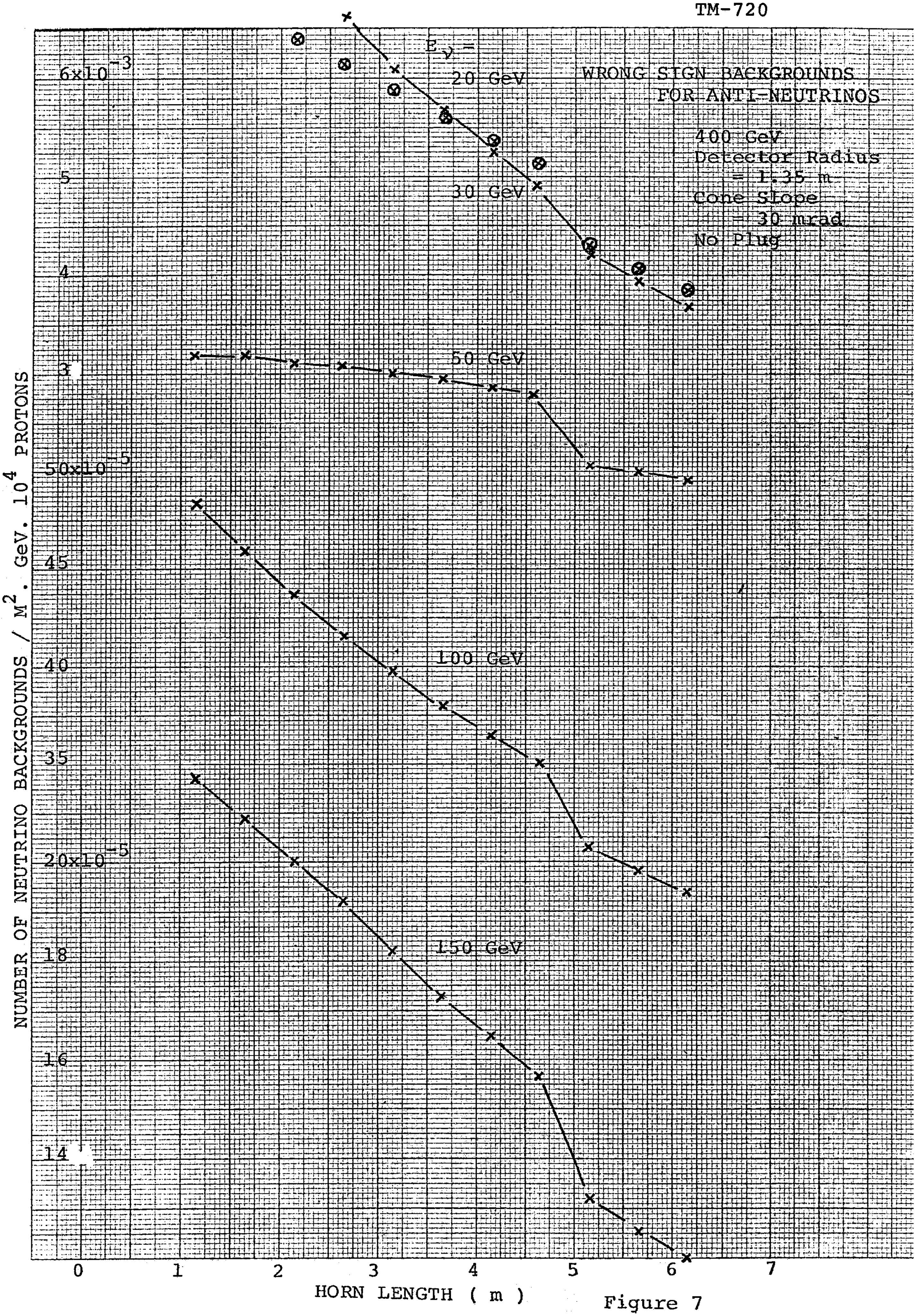
WRONG SIGN BACKGROUNDS
FOR ANTI-NEUTRINOS
400 GeV
Detector Radius
= 1.35 m
Cone Slope
= 30 mrad
No Plug
E_ν =
20 GeV
30 GeV
50 GeV
100 GeV
150 GeV
6×10^{-3}
5
4
3
50×10^{-5}
45
40
35
20×10^{-5}
18
16
14
0
1
2
3
4
5
6
7
NUMBER OF NEUTRINO BACKGROUNDS / M^2 . GeV. 10^4 PROTONS
HORN LENGTH (m)

Figure 7

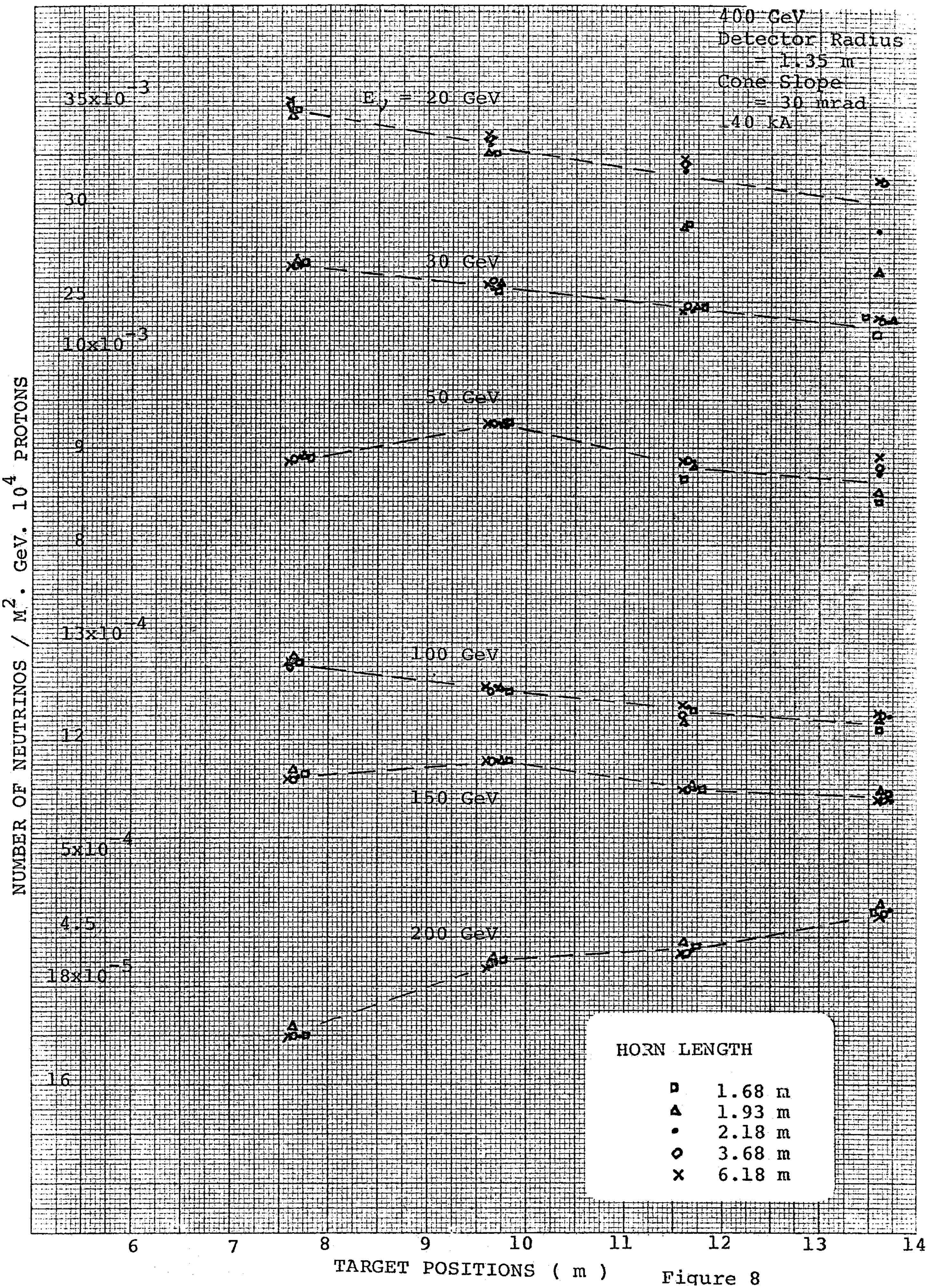
400 GeV
Detector Radius
= 1.35 m
Cone Slope
= 30 mrad
140 kA
E_ν = 20 GeV
30 GeV
50 GeV
100 GeV
150 GeV
200 GeV
35x10^{-3}
30
25
10x10^{-3}
9
8
13x10^{-4}
12
5x10^{-4}
4.5
18x10^{-5}
16
NUMBER OF NEUTRINOS / M^2 . GeV. 10^4 PROTONS
6
7
8
9
10
11
12
13
14
TARGET POSITIONS (m)
HORN LENGTH
1.68 m
1.93 m
2.18 m
3.68 m
6.18 m

Figure 8

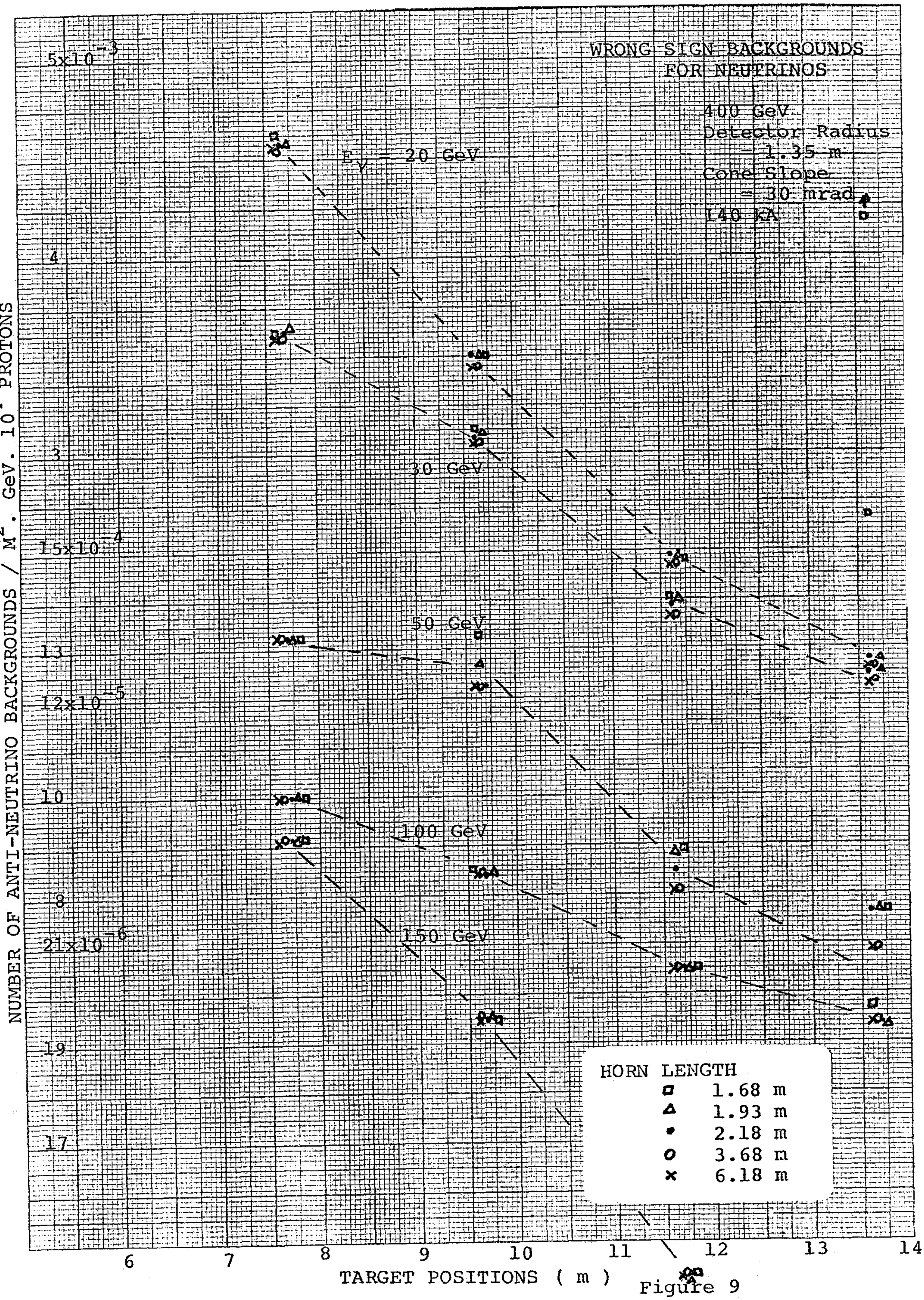
WRONG SIGN BACKGROUNDS FOR NEUTRINOS
400 GeV
Detector Radius = 1.35 m
Cone Slope = 30 mrad
140 kA
E_ν = 20 GeV
30 GeV
50 GeV
100 GeV
150 GeV
HORN LENGTH
□ 1.68 m
△ 1.93 m
• 2.18 m
o 3.68 m
x 6.18 m
NUMBER OF ANTI-NEUTRINO BACKGROUNDS / M^2. GeV. 10^4 PROTONS
TARGET POSITIONS (m)
5×10^{-3}
4
3
15×10^{-4}
13
12×10^{-5}
10
8
21×10^{-6}
19
17
6
7
8
9
10
11
12
13
14

Figure 9

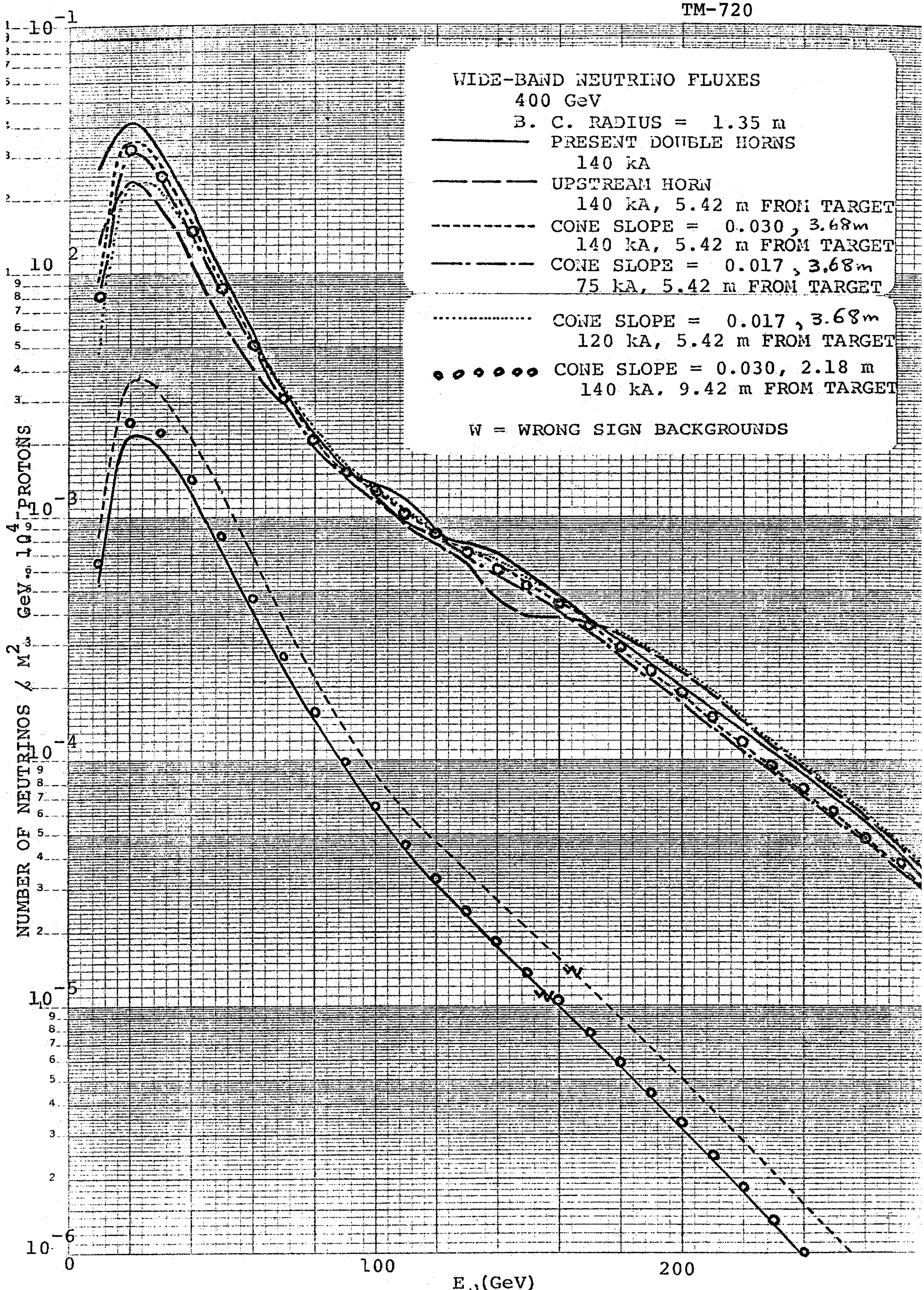
WIDE-BAND NEUTRINO FLUXES
400 GeV
B. C. RADIUS = 1.35 m
PRESENT DOUBLE HORNS
140 kA
UPSTREAM HORN
140 kA, 5.42 m FROM TARGET
CONE SLOPE = 0.030, 3.68m
140 kA, 5.42 m FROM TARGET
CONE SLOPE = 0.017, 3.68m
75 kA, 5.42 m FROM TARGET
CONE SLOPE = 0.017, 3.68m
120 kA, 5.42 m FROM TARGET
CONE SLOPE = 0.030, 2.18 m
140 kA, 9.42 m FROM TARGET
W = WRONG SIGN BACKGROUNDS
W
W
NUMBER OF NEUTRINOS / M² GeV. 10⁹ PROTONS
10⁻²
10⁻³
10⁻⁴
10⁻⁵
10⁻⁶
0
100
200
E_ν(GeV)

Figure 10

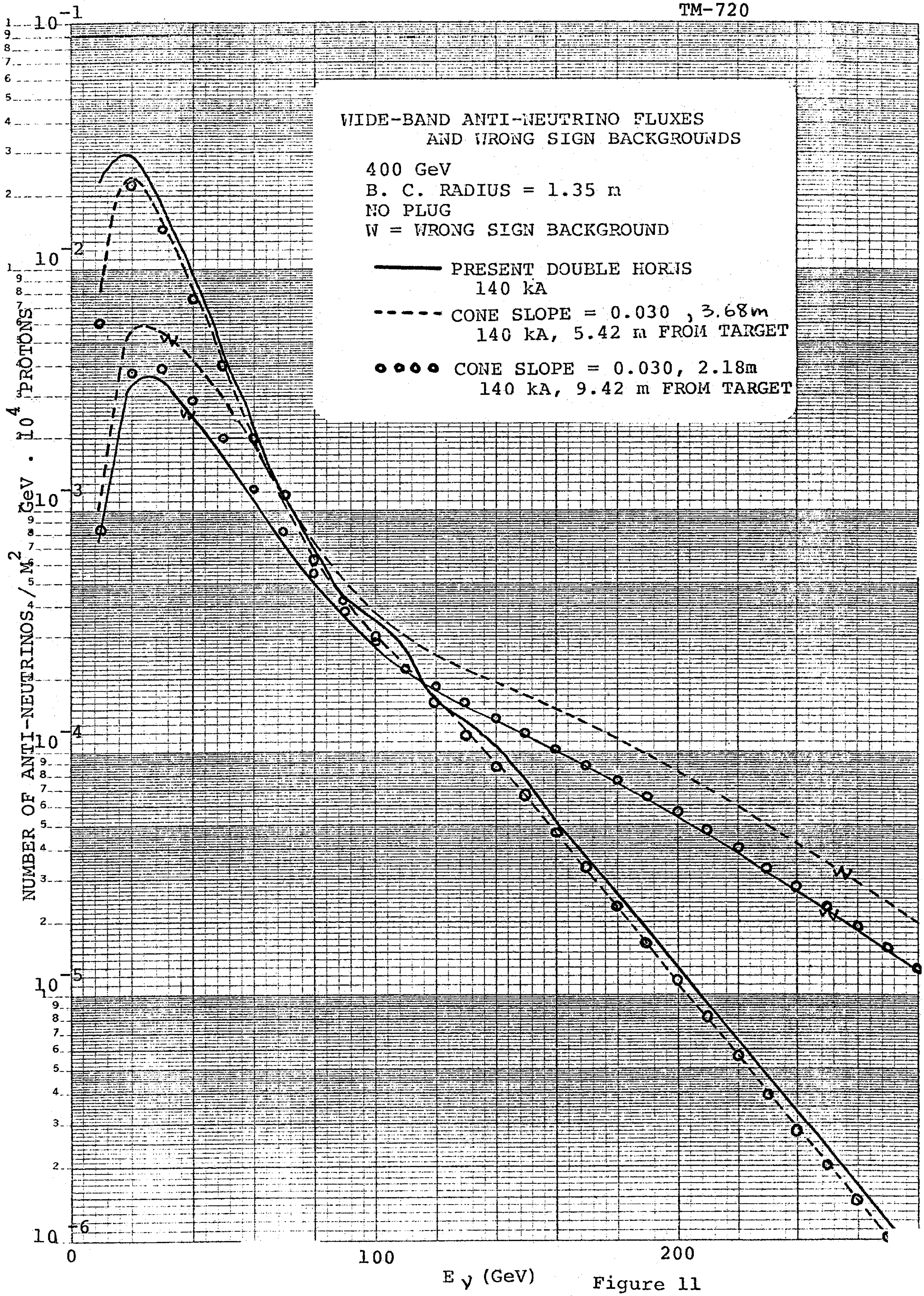
WIDE-BAND ANTI-NEUTRINO FLUXES
AND WRONG SIGN BACKGROUNDS
400 GeV
B. C. RADIUS = 1.35 m
NO PLUG
W = WRONG SIGN BACKGROUND
PRESENT DOUBLE HORNS
140 kA
CONE SLOPE = 0.030 , 3.68m
140 kA, 5.42 m FROM TARGET
CONE SLOPE = 0.030, 2.18m
140 kA, 9.42 m FROM TARGET
NUMBER OF ANTI-NEUTRINOS / M² · GeV · 10⁴ PROTONS
E γ (GeV)
0
100
200
10⁻¹
10⁻²
10⁻³
10⁻⁴
10⁻⁵
10⁻⁶
W

Figure 11

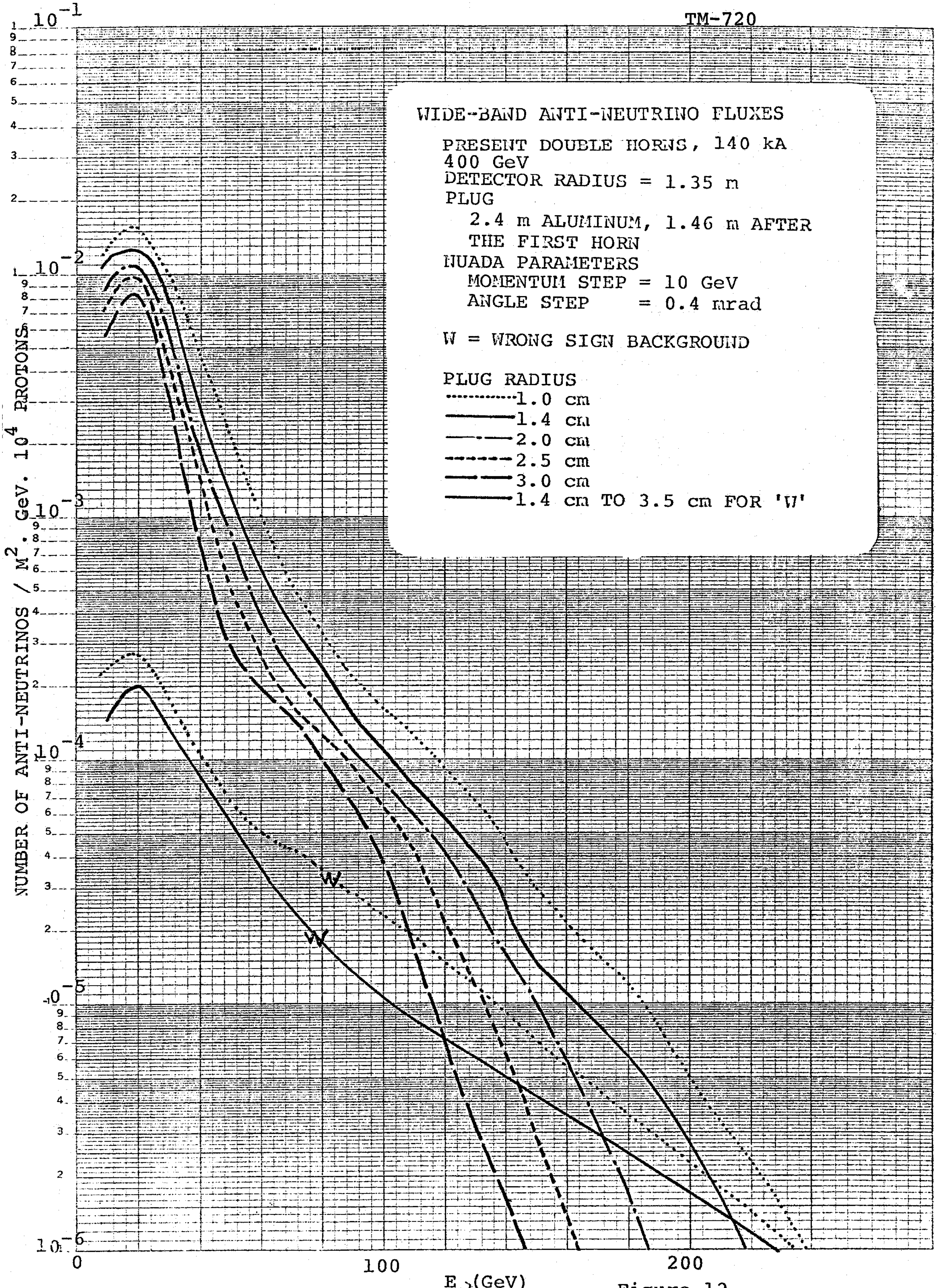

WIDE-BAND ANTI-NEUTRINO FLUXES
PRESENT DOUBLE HORNS, 140 kA
400 GeV
DETECTOR RADIUS = 1.35 m
PLUG
2.4 m ALUMINUM, 1.46 m AFTER THE FIRST HORN
NUADA PARAMETERS
MOMENTUM STEP = 10 GeV
ANGLE STEP = 0.4 mrad
W = WRONG SIGN BACKGROUND
PLUG RADIUS
1.0 cm
1.4 cm
2.0 cm
2.5 cm
3.0 cm
1.4 cm TO 3.5 cm FOR 'W'
W
W
NUMBER OF ANTI-NEUTRINOS / M². GeV. 10⁴ PROTONS
10^{-1}
10^{-2}
10^{-3}
10^{-4}
10^{-5}
10^{-6}
0
100
200
E_ν(GeV)

Figure 12

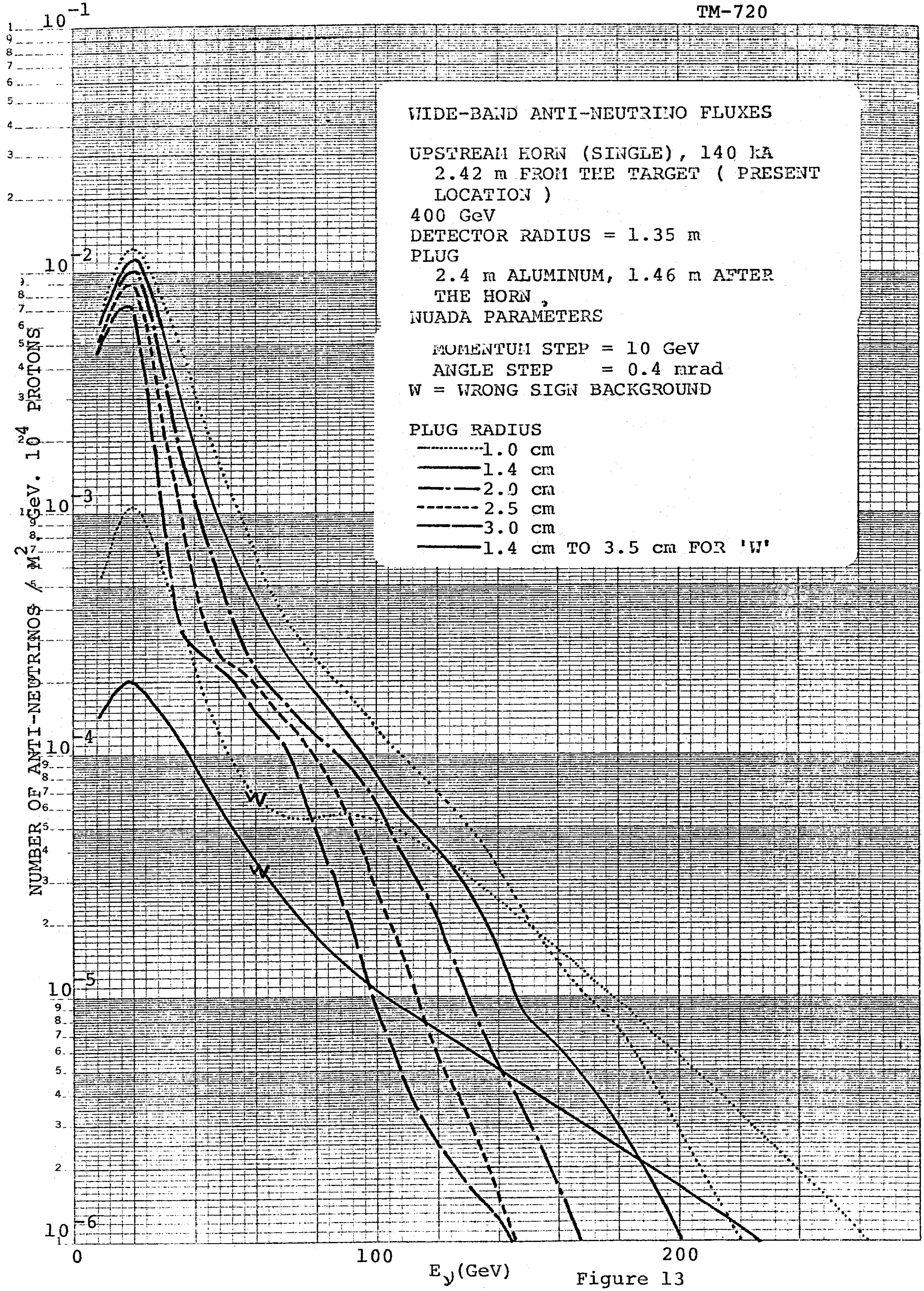
WIDE-BAND ANTI-NEUTRINO FLUXES
UPSTREAM HORN (SINGLE), 140 kA
2.42 m FROM THE TARGET (PRESENT LOCATION)
400 GeV
DETECTOR RADIUS = 1.35 m
PLUG
2.4 m ALUMINUM, 1.46 m AFTER THE HORN,
NUADA PARAMETERS
MOMENTUM STEP = 10 GeV
ANGLE STEP = 0.4 mrad
W = WRONG SIGN BACKGROUND
PLUG RADIUS
1.0 cm
1.4 cm
2.0 cm
2.5 cm
3.0 cm
1.4 cm TO 3.5 cm FOR 'W'
W
W
NUMBER OF ANTI-NEUTRINOS / M^2 GeV. 10^4 PROTONS
10^{-1}
10^{-2}
10^{-3}
10^{-4}
10^{-5}
10^{-6}
0
100
200
$E_{\bar\nu}$(GeV)

Figure 13

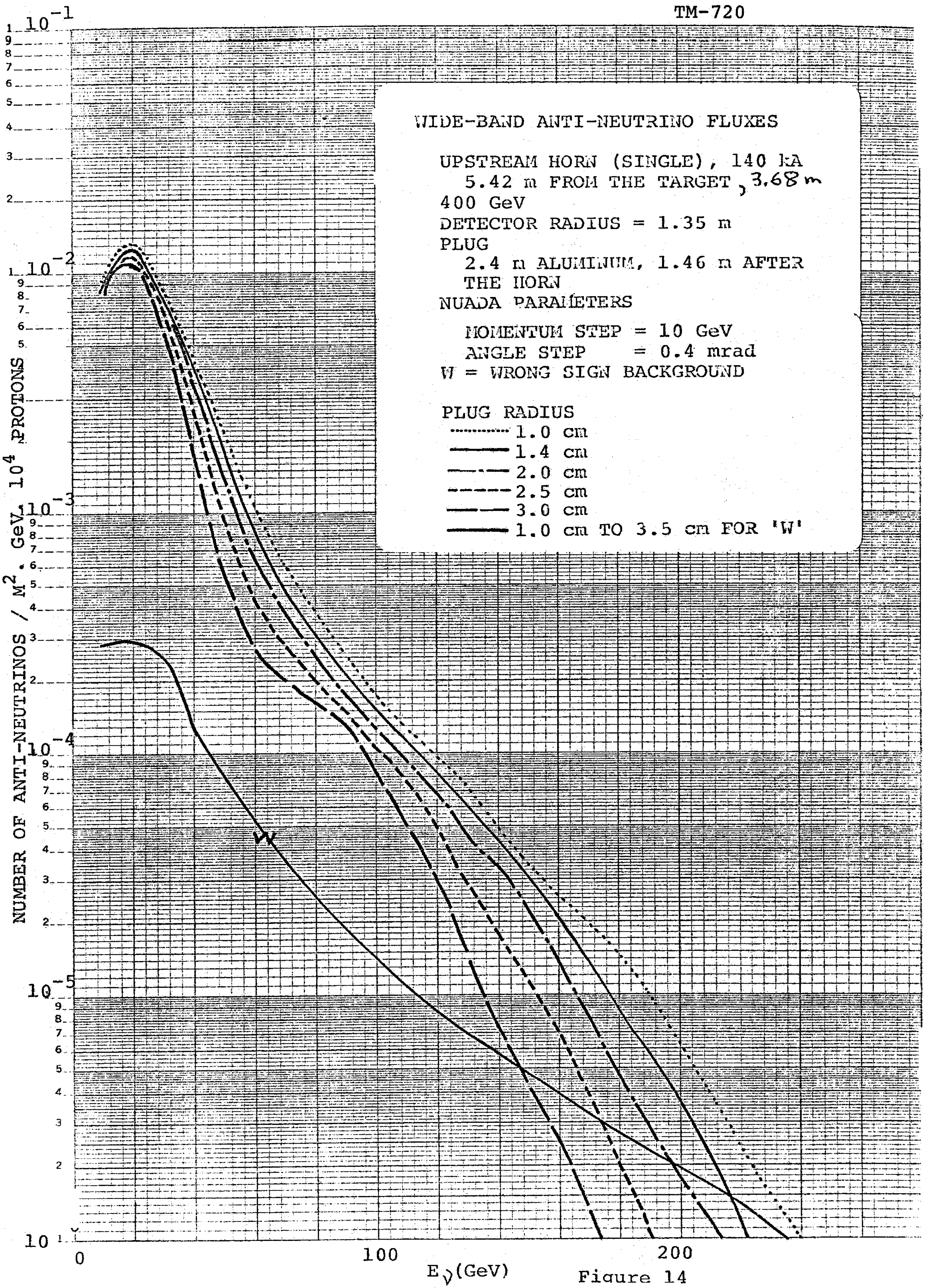
WIDE-BAND ANTI-NEUTRINO FLUXES
UPSTREAM HORN (SINGLE), 140 kA
5.42 m FROM THE TARGET, 3.68 m
400 GeV
DETECTOR RADIUS = 1.35 m
PLUG
2.4 m ALUMINUM, 1.46 m AFTER THE HORN
NUADA PARAMETERS
MOMENTUM STEP = 10 GeV
ANGLE STEP = 0.4 mrad
W = WRONG SIGN BACKGROUND
PLUG RADIUS
1.0 cm
1.4 cm
2.0 cm
2.5 cm
3.0 cm
1.0 cm TO 3.5 cm FOR 'W'
W
NUMBER OF ANTI-NEUTRINOS / M2 . GeV . 10^4 PROTONS
E_ν (GeV)
0
100
200
10^-1
10^-2
10^-3
10^-4
10^-5
10

Figure 14

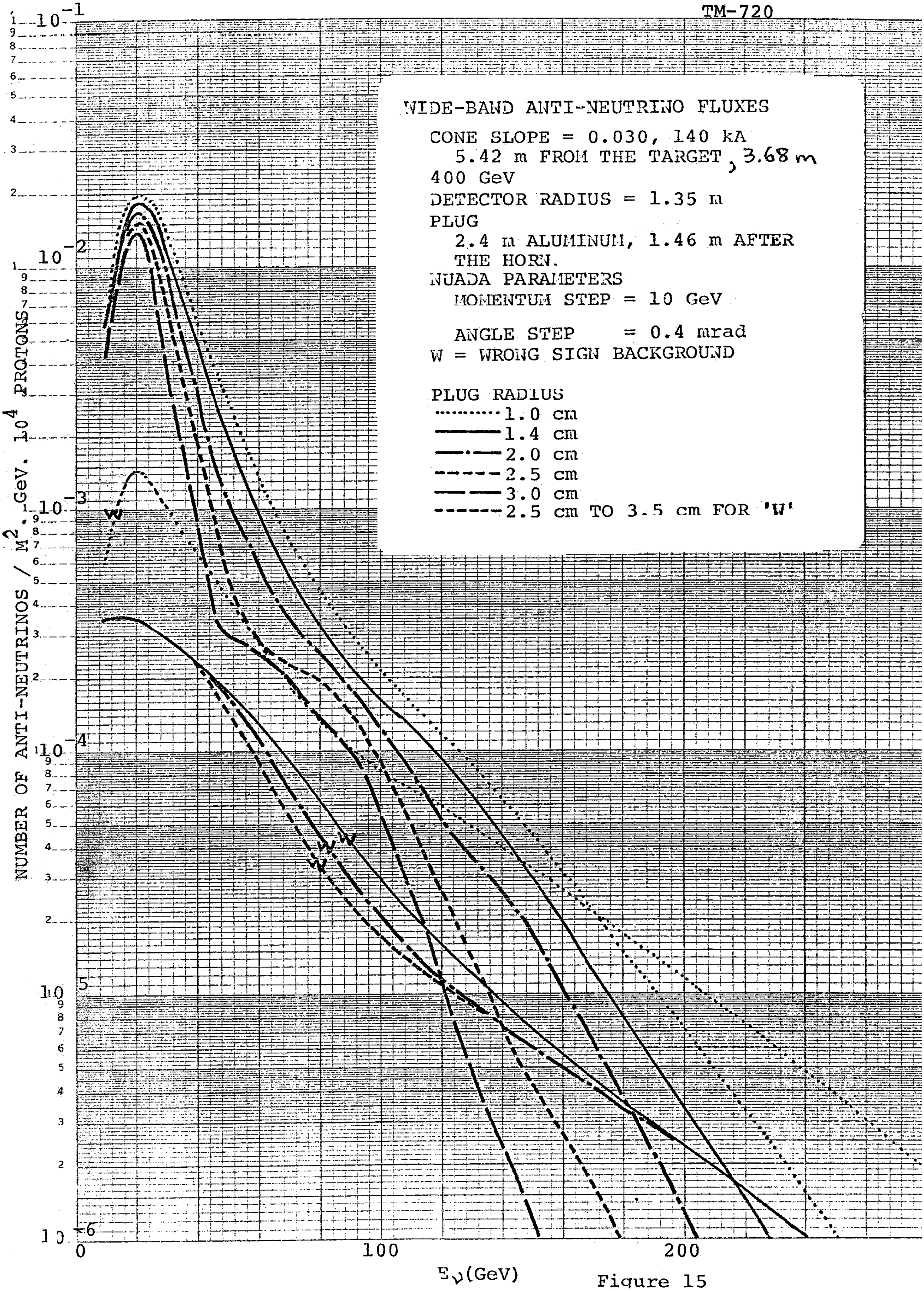
WIDE-BAND ANTI-NEUTRINO FLUXES
CONE SLOPE = 0.030, 140 kA
5.42 m FROM THE TARGET, 3.68 m
400 GeV
DETECTOR RADIUS = 1.35 m
PLUG
2.4 m ALUMINUM, 1.46 m AFTER THE HORN.
NUADA PARAMETERS
MOMENTUM STEP = 10 GeV
ANGLE STEP = 0.4 mrad
W = WRONG SIGN BACKGROUND
PLUG RADIUS
1.0 cm
1.4 cm
2.0 cm
2.5 cm
3.0 cm
2.5 cm TO 3.5 cm FOR 'W'
NUMBER OF ANTI-NEUTRINOS / M^2. GeV. 10^4 PROTONS
E_ν(GeV)
0
100
200
10^{-1}
10^{-2}
10^{-3}
10^{-4}
10^{-5}
10^{-6}
W

Figure 15

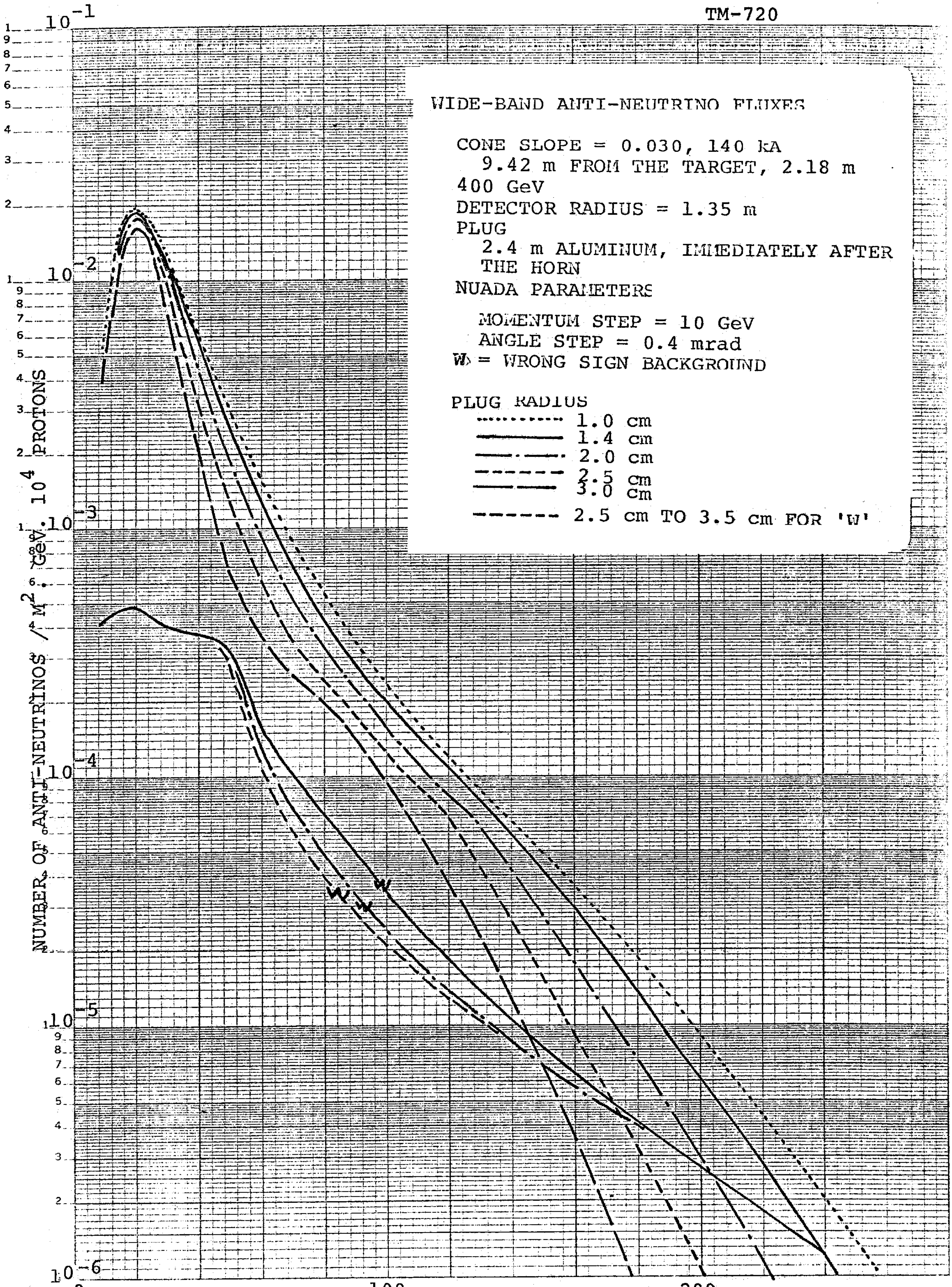
WIDE-BAND ANTI-NEUTRINO FLUXES
CONE SLOPE = 0.030, 140 kA
9.42 m FROM THE TARGET, 2.18 m
400 GeV
DETECTOR RADIUS = 1.35 m
PLUG
2.4 m ALUMINUM, IMMEDIATELY AFTER THE HORN
NUADA PARAMETERS
MOMENTUM STEP = 10 GeV
ANGLE STEP = 0.4 mrad
W = WRONG SIGN BACKGROUND
PLUG RADIUS
1.0 cm
1.4 cm
2.0 cm
2.5 cm
3.0 cm
2.5 cm TO 3.5 cm FOR 'W'
W
W
W
NUMBER OF ANTI-NEUTRINOS / M² GeV 10⁴ PROTONS
E (GeV)
0
100
200
10⁻¹
10⁻²
10⁻³
10⁻⁴
10⁻⁵
10⁻⁶

Figure 16

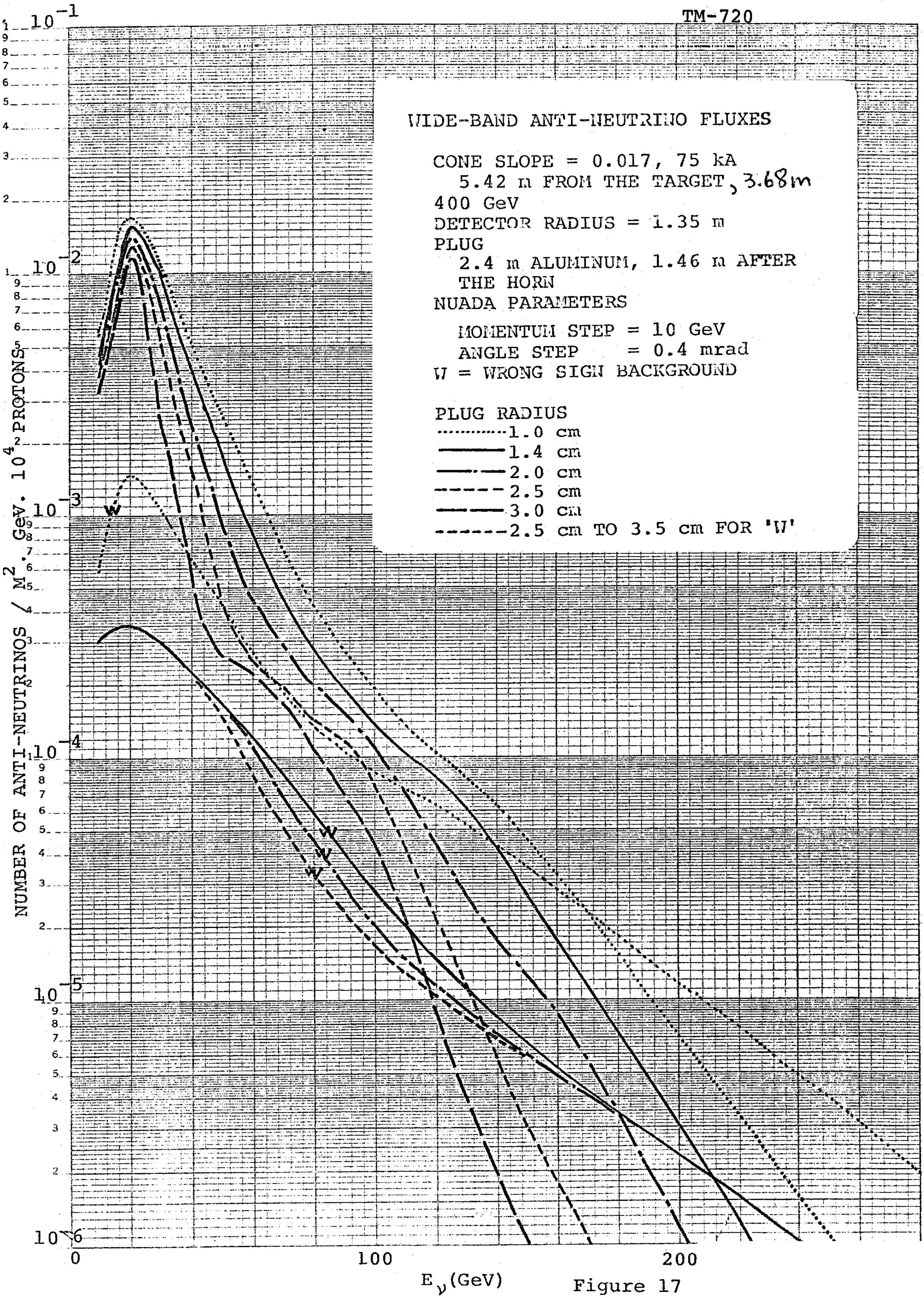
WIDE-BAND ANTI-NEUTRINO FLUXES
CONE SLOPE = 0.017, 75 kA
5.42 m FROM THE TARGET, 3.68m
400 GeV
DETECTOR RADIUS = 1.35 m
PLUG
2.4 m ALUMINUM, 1.46 m AFTER THE HORN
NUADA PARAMETERS
MOMENTUM STEP = 10 GeV
ANGLE STEP = 0.4 mrad
W = WRONG SIGN BACKGROUND
PLUG RADIUS
1.0 cm
1.4 cm
2.0 cm
2.5 cm
3.0 cm
2.5 cm TO 3.5 cm FOR 'W'
NUMBER OF ANTI-NEUTRINOS / M^2. GeV. 10^4 PROTONS
10^{-1}
10^{-2}
10^{-3}
10^{-4}
10^{-5}
10^{-6}
0
100
200
E_ν(GeV)

Figure 17